



Graphene and Graphene-Like Materials as a Sensor for CO Gas

Zainab Jassim Mohammed*^{ID}, Nidhal Mohammed O. Al Shareefi^{ID}, Musa Kadhim Mohsin^{ID}

Department of Physics, College of Science, University of Babylon, Hilla 51001, Iraq

Corresponding Author Email: sci850.zanab.jasem@student.uobabylon.edu.iq

Copyright: ©2025 The authors. This article is published by IIETA and is licensed under the CC BY 4.0 license (<http://creativecommons.org/licenses/by/4.0/>).

<https://doi.org/10.18280/rcma.350102>

ABSTRACT

Received: 1 August 2024

Revised: 3 September 2024

Accepted: 6 February 2025

Available online: 28 February 2025

Keywords:

silicene, boron nitride, graphene, gallium, arsenic, DFT

Carbon monoxide (CO) is a very poisonous air pollutant that is generated when fuels are not completely burned. Due to its lack of colour and scent, carbon monoxide (CO) is hazardous and poses a significant danger. As a result, it is necessary to have CO sensors. Gas sensing applications have employed many two-dimensional (2D) materials, including graphene, silicene, and BN. The addition of dopants or defects significantly increases the sensitivity of graphene-based gas sensors. This study employed Density Functional Theory (DFT) to examine the adsorption mechanisms of pristine and (Ga, As)-doped graphene, silicene, and boron nitride on the toxic gas CO. The calculations involved determining the adsorption energy, adsorption distance, charge transfer, sensitivity, and density of states. The findings indicate that introducing Ga atoms into G/S/BN ribbons greatly enhances the adsorption energy, but pure ribbons have very low adsorption energy to CO gas, indicating weak physical adsorption. The best sensitivity, BN-DopeAs, reaches (202.941%), while BN-DopGa has the highest adsorption energy (817.941). The results indicate that BN doped with (Ga, As) atoms is most suitable for CO sensing applications.

1. INTRODUCTION

Carbon monoxide (CO) is a very poisonous air pollutant that is generated when fuels are burned incompletely. It is frequently present in automotive emissions, as well as in the combustion of household fuels. Due to its lack of color and scent, this substance is both highly poisonous and incredibly hazardous [1]. So, it is imperative to install carbon monoxide sensors in various settings, including the detection of slow-burning fires and the monitoring of air quality in urban and enclosed environments [2]. The sensing material is an essential part of the gas sensor device [3, 4]. Gas sensing applications have employed many two-dimensional (2D) materials, including graphene, silicene, and BN. The materials are selected based on their outstanding stability, distinctive structural properties, large specific surface area, excellent volume ratio, low power usage, and commendable adsorption capability [5, 6]. However, graphene has significant limitations, one of which is the lack of a band gap [7, 8], The inadequate structural stability of silicene [9], Furthermore, the exceptional chemical inertness of boron nitride [10], which limit their utilization in gas sensing applications. Currently, the most practical approach to regulate the semiconductor properties of graphene is through atomic doping. Research has shown that the sensitivity of graphene-based gas sensors can be greatly enhanced by introducing dopants or defects [11].

The study of gas adsorption on pure and (Ga, As) doped graphene, silicene, and boron nitride nano-ribbons reveals significant enhancements in sensitivity and adsorption energy

due to doping. This has implications for the development of advanced gas sensors. Pure graphene exhibits weak adsorption energies for gases like NH_3 and NO_2 , while Ga-doped graphene shows significantly increased adsorption energies, particularly for NO_2 , due to strong orbital hybridization and charge transfer, with values reaching -1.928 eV [12]. Also, doping with Ga or As modifies the electronic properties, enhancing the sensitivity of the material to various gases. For instance, Ga-doped graphene opens a band gap of 0.267 to 0.397 eV, improving gas detection capabilities [12]. Similar trends are observed in boron nitride nanotubes, where doping increases adsorption energy for harmful gases like H_2SiCl_2 , indicating a stronger interaction compared to pristine structures [13]. While specific studies on silicene were not highlighted, its structural similarities to graphene suggest potential for enhanced gas sensing through doping. In conclusion, doping graphene and related materials significantly enhances their gas adsorption capabilities, making them promising candidates for sensor applications.

The present theoretical study aims to study of the structural and electronic properties of pure and doped graphene, silicene and boron nitride and investigate the possibility of using this nano-ribbons as a detector for carbon monoxide (CO) gas. through the occurrence of adsorption between nano-ribbons and gas molecules. This is done by using the graphene, silicene, and boron nitride nano-ribbons in the pure state. Then study the doping of these structure with (Ga, As) atoms to know the effect of this on adsorption.

2. MATERIALS AND METHODS

The calculations in this work were conducted using unrestricted DFT theory, which was chosen for its high precision in determining the structural and electronic properties. We have selected the functional B3LYP with the 6-31G basis set at ground state, which is implemented in the Gaussian 09 software package. The B3LYP Functional is widely recognized for its effectiveness in predicting electronic properties and spectra, particularly in coordination complexes [14]. Also, the 6-31G basis set, enhances the accuracy of DFT calculations by better representing electron distribution [15]. The combination of B3LYP with the 6-31G basis set allows for efficient calculations without significant loss of accuracy [16]. Also, TD-DFT was used to compute UV-visible.

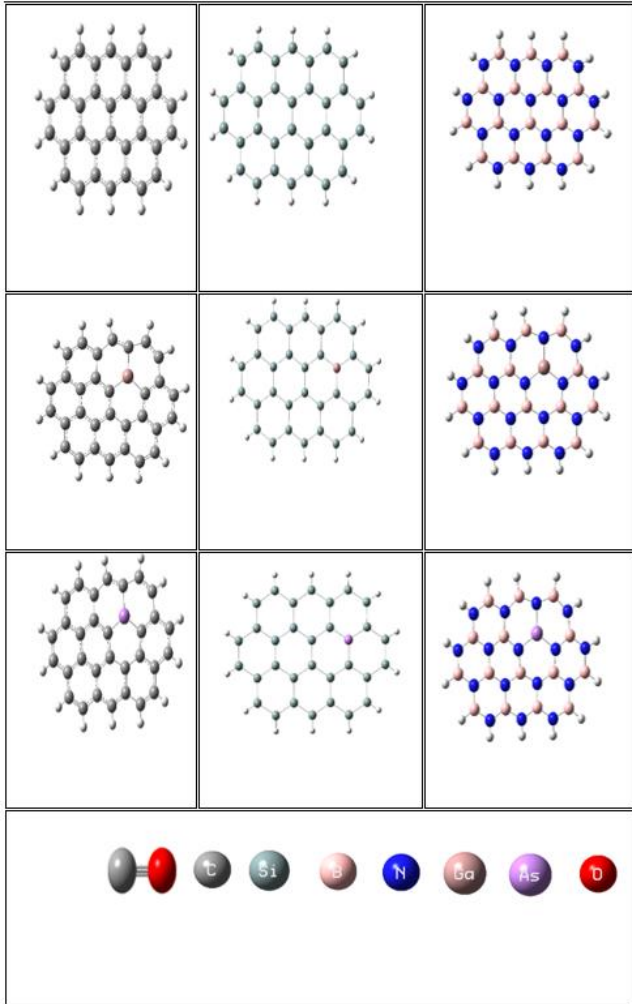


Figure 1. Optimization structure of student nano ribbons and CO gas

We utilized graphene, silicene, and boron nitride nanoribbons, each composed of 46 atoms (32 carbon/silicon for graphene/silicene and 16 boron/nitrogen for boron nitride, together with 14 hydrogen atoms). Additionally, we substituted a carbon/silicon/nitrogen atom with a gallium/arsenic atom that has been doped, and then we attached a single carbon monoxide molecule to it. The dopant concentration that corresponds to this value is roughly 2.17% in pure G-NR. The bond lengths for C=C, C-C (aromatic), and C-H in GR ribbon are 1.375, 1.4195, and 1.086 Å, in that order. For (C=C=C) and (C=C-H), the angles between the

atoms are specified as (120.244) and (120.306) degrees, respectively, the result shows that agreement with a previous study [17]. For pure S-NR, the bond lengths for Si-Si and Si-H in the SR ribbon are (2.247) and (1.496) Å, respectively. The (Si-Si-Si) and (Si-Si-H) atoms have angles of (120.486) and (119.440) degrees, respectively, the result shows that agreement with a previous study [18]. The bond lengths for B-N, (N-H), and (B-H) on the pure BN-NR are (1.443), (1.012), and (1.191) Å, in that order. Atoms N-B-N and B-N-B have respective angles of (120.675) and (121.311) degrees, the result shows that agreement with a previous study [19]. The geometrical structure of the ribbons under investigation is shown in Figure 1.

To further investigate the electronic conductivity and chemical stability of (Ga, As) doped G/S/BN-NR and the adsorption system, we use Eq. 1 to determine E_g (energy gap) between the (HOMO) and (LUMO).

$$E_g = E_{LUMO} - E_{HOMO} \quad (1)$$

The representation of the lowest unoccupied molecular orbit (E_{LUMO}) and the highest occupied molecular orbit (E_{HOMO}) is indicated [20].

Quantum descriptors encompass several properties such as ionization potential (IP), and electron affinity (EA), which can be derived from Eqs. (2) and (3).

$$IP = -E_{HOMO} \quad (2)$$

$$EA = -E_{LUMO} \quad (3)$$

Eq. (4) calculates the energy of adsorption (E_a) by subtracting the sum of the molecule's energy (in gas phase) and the energy of pure doped G/S/BN-NR from the total energy of the system (including gas and Ribbon) [21].

$$E_a = E_{total} - (E_{Ribbon} + E_{gas}) \quad (4)$$

The energy of adsorption is a scientific word that quantifies the strength of adsorption. It is usually expressed as a negative value, and when it becomes positive, adsorption becomes unstable. The system's stability increases as the magnitude of the energy of adsorption increases. Smaller ones usually indicate the instability of adsorption.

The charge transfer (Q) between the gas molecules and the CO- Nano ribbon is calculated using analysis of hirshfeld charges.

$$Q = Q_{adsorbed} - Q_{isolated} \quad (5)$$

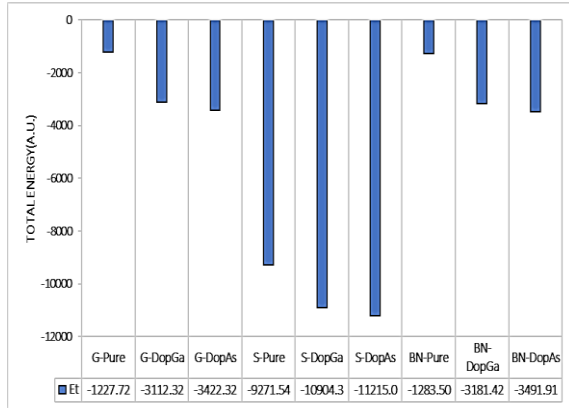
In this scenario, $Q_{adsorbed}$ represents the electric charge of the gas molecules when they are adsorbed, while $Q_{isolated}$ refers to the charge of the gas molecules after they have been isolated. The transfer of electrons between gas molecules and the adsorbent surface is denoted by positive Q [22]. Eq. 6 can be used to determine the sensor's sensitivity (S).

$$S = \left(\frac{|E_g(1) - E_g(0)|}{E_g(0)} \right) * 100\% \quad (6)$$

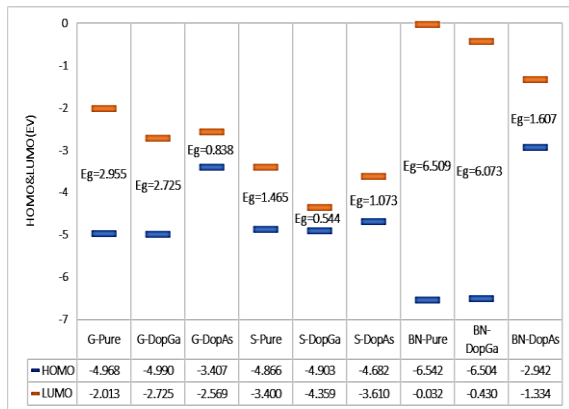
$E_g(1)$ represents the energy gap in the presence of gas, $E_g(0)$ represents the energy gap in the absence of gas, and S denotes sensitivity [17].

3. RESULTS AND DISCUSSION

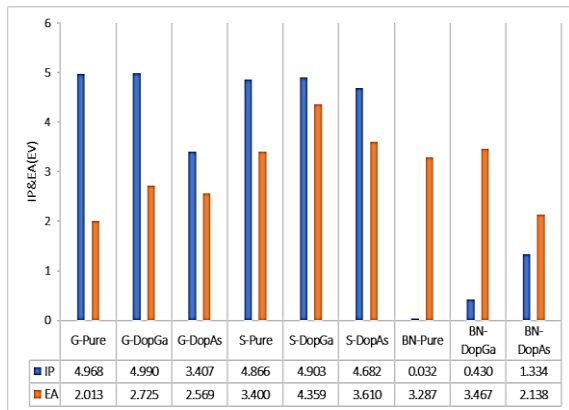
3.1 Electronic properties of the studied nano-ribbons



(a) Total energy



(b) HOMO&LUMO



(c) IP&EA

Figure 2. Electronic properties of studied nano-ribbons

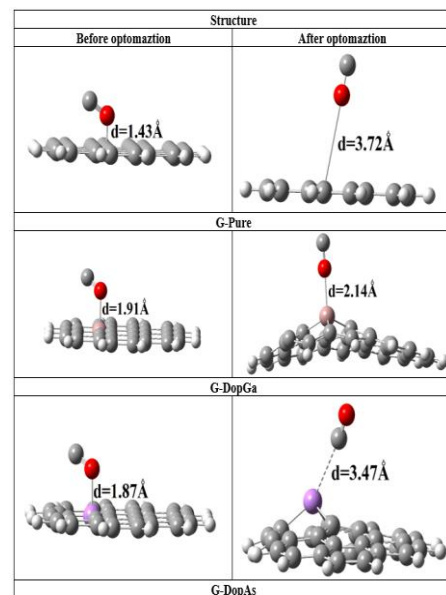
As a reflection of each structure's binding energy, the data shown in Figure 2(a) demonstrates that doping resulted in a decrease in total energy, where total energy is defined as the total energy of the ground state which is approximately the sum of the ground state energy of all atoms in each structure [23], indicating that these nano-ribbons have good relaxing. Where adding atoms leads to modifying the structure of the electronic bands, which affects the energy distribution in the material and leads to a decrease in the total energy. Energy band gap found by Eq. (1). The band gap refers to energy difference between the highest occupied molecular orbital and lowest unoccupied molecular orbital. Figure 2(b) shown the

energy gap of the studied nano-ribbons, The Pure and doped G/S nano-ribbons were a semiconductor material whereas pure BNR was an insulator material, doping with an As atom reduced the energy gap of graphene by 2.118, the reason for such an outcome can be found in the small polarization induced by the doped nano-ribbon [24]. Also, doping BNR with (As) atom significantly reduces the energy gap and turns the material into a semiconductor, as it creates energy levels located between the HOMO-LUMO levels, facilitates the electronic transition between the valence and conduction bands.

The results of ionization energy IE and electron affinity EA are shown in Figure 2(c). These properties are critical in determining the ability to distinguish or escape electrons between doping systems [25]. Clearly figure shows that the BN-Pure has the highest ionization energy value when compared with the G/S nano-ribbons. The ionization energy of BN-DopAs is lower than that of other nano-ribbons. This suggests that BN-DopAs have a greater ability to donate an electron to form a cation than the others. In comparison to other nano-ribbons, S-DopGa nano-ribbon have the highest EA value because they have a high electron acceptability to become anion. The electron affinity of the BN-pure is small because it is an insulator and stable and does not interact with the environment, and when Ga was added, the affinity increased, but when as were added, the affinity increased more, meaning that it became freer to interact with the environment, and this is due to the presence of abundance of electrons As nano-particles [26].

3.2 The adsorption energies of the examined configurations for the CO gas molecule

The distance between the CO gas and the different nano-ribbons is calculated by optimizing the pure and doped G/S/BN-NR. The pure and modified G/S/BN layers' surfaces are precisely where the carbon monoxide (CO) gas molecules are found. As it has been shown in Figure 3. After optimization, we noticed changes in the arrangement of multiple nano ribbons and the distance between the gas molecules and the nano ribbons. Figure 3 demonstrates that the G/BN, doped with Ga/As atoms, displays a significant interaction with the gas.



(a) G-NR

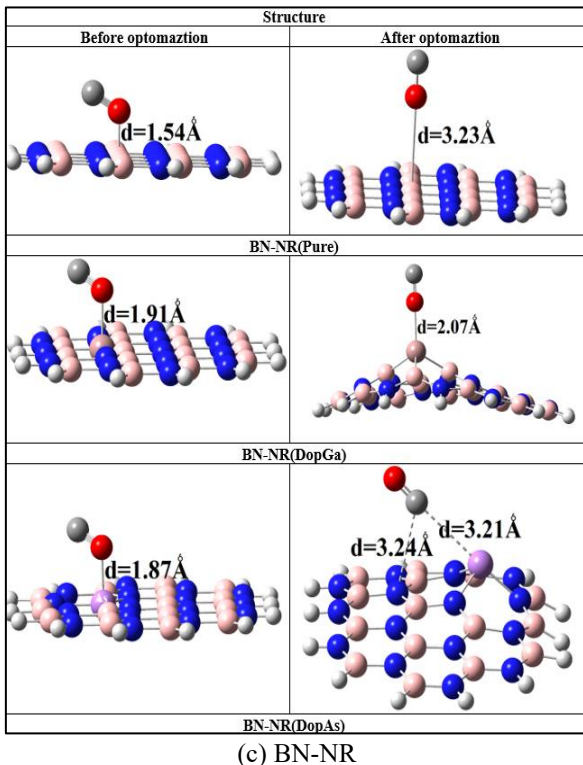
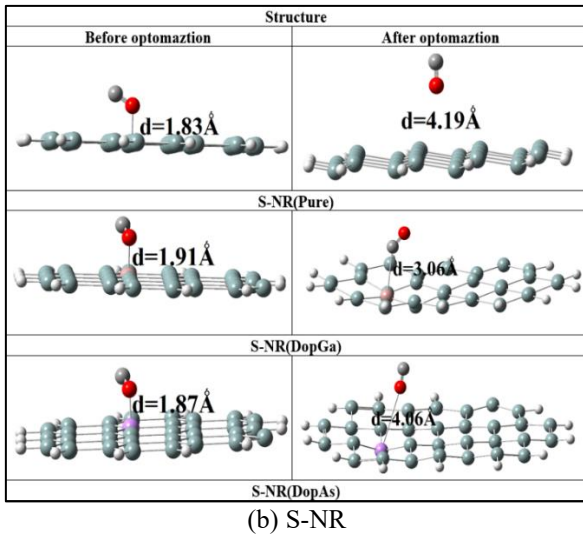


Figure 3. Adsorption of CO gas molecule by G/S/BN-NR pure and doped (Ga, As) ball-and-stick model

Table 1 demonstrates that the adsorption energy investigations reveal negligible adsorption energy of CO gas on pure G/S/BN-NR. This indicates poor physical adsorption, independent of the CO gas composition. Meeting the gas adsorption requirements became difficult as a result of the low adsorption energy. Subsequently, we employed CO gas adsorption on the models that were doped with (Ga, As) atoms. The computed results of the adsorption energy indicated that the presence of Ga atoms significantly increased the adsorption capacity of graphene and Boron nitride. Conversely, the adsorption energy maintained at a low level for G/S/BN doped with As atoms. The adsorption energy of BN_DopGa is 817.491 eV, which surpasses the adsorption energy of BN-NR doped with metal atoms (Co, P) determined by Milon et al. [27]. Strong hybridization between the carbon p with gallium d orbitals is responsible for the CO molecule's adsorption on the gallium-doped BN [28]. In this instance, the Ga site's

attraction energy for CO is greater than that of the As site with a comparable arrangement, which leads to an increase in effective adsorption sites on the BN-NR surface, where gallium can interact with molecules through covalent bonds [29].

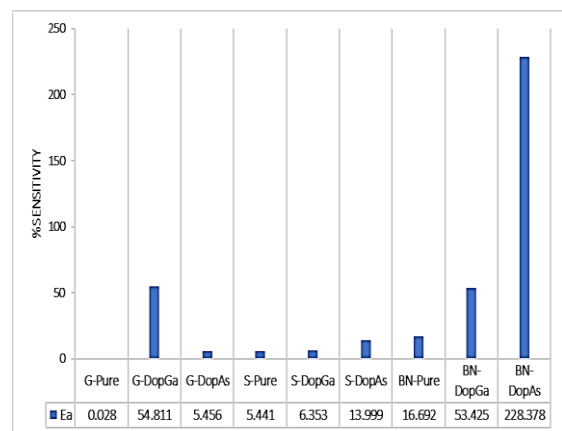
Table 1. The energies of adsorption

Structure	E_a (eV)
G-Pure	0
G-DopGa	18.517
G-DopAs	-1.605
S-Pure	-0.383
S-DopGa	-0.413
S-DpAs	-0.421
BN-Pure	-0.029
BN-DopGa	817.491
BN-DopAs	-5.61

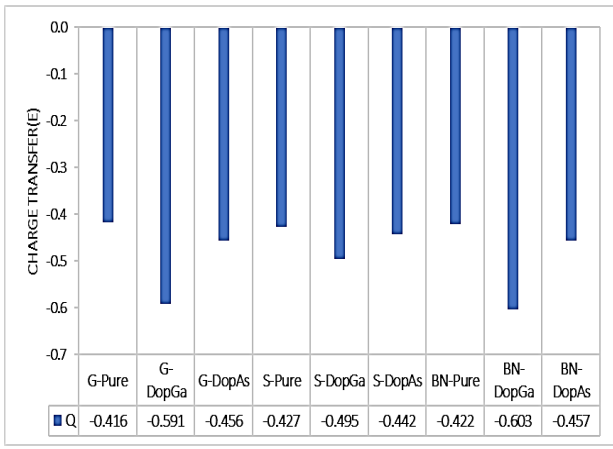
3.3 The charge transfer and sensitivity of the investigated Ribbons

To test the gas sensing capabilities of pure and doped nano ribbons, it is necessary to measure the sensitivity of gases that interact with their surfaces [30]. In its pure form, G/S/BN-NR has made CO gas-sensitive; when doped with Ga or As, the gas sensitivity increases. The sensitivity of G/BN-NR is significantly enhanced by the Ga atom, Gallium doping enhances adsorption interactions between the surface of the nanoribbons and CO molecules. This enhanced adsorption increases the material's response to changes in CO gas concentration, which increases the material's sensitivity to gas detection. As it has been shown in Figure 4(a), The BN_DopAs atom has a maximum doping-induced sensitivity value of 242.721. That's because Arsenic doping adds new energy states within the electronic structure of the BN nanoribbons, narrowing the energy gap. This increases the interaction of the material with the presence of gas molecules by enhancing charge transfer between the gas and the nanoribbon.

This theory is further bolstered by the charge transfer data presented in Figure 4(b). Charge population analysis shows that there is only a little amount of charge transferred from Pure G/S/BN-NR to CO, with values of -0.416e/-0.426/-0.421. However, the amount of charge transfer increases significantly after doping. Negative charge transfer refers which involves electrons moving from the Nanoribbon's surface to the gas molecule [22]. Depending on the grafting procedure, the amount of charge transfer could vary.



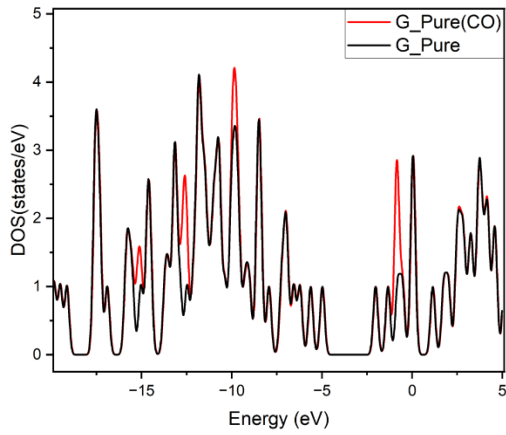
(a) Sensitivity



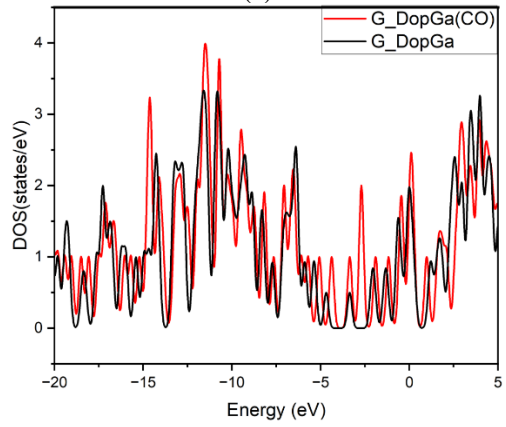
(b) Charge Transfer

Figure 4. The sensitivity and adsorption energy for studied structures

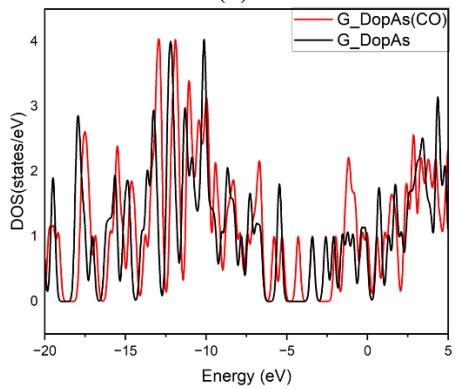
3.4 Density of states (DOS)



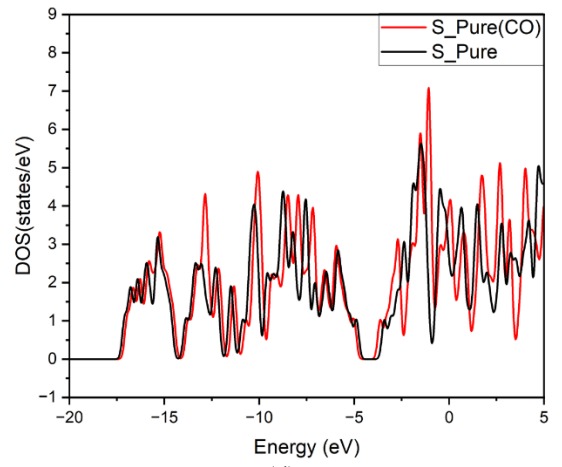
(a)



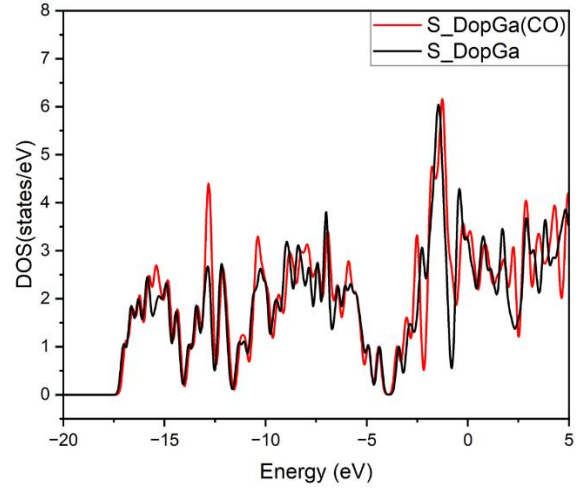
(b)



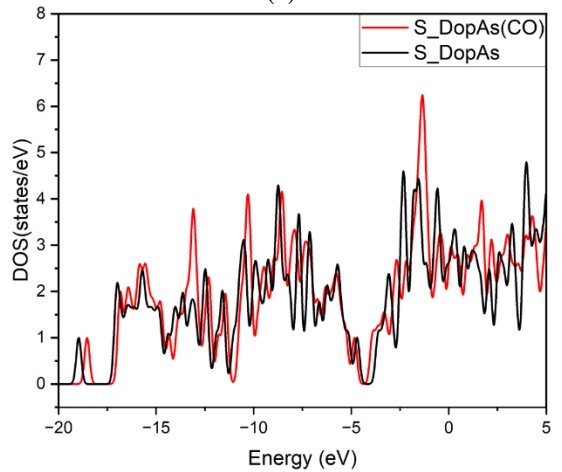
(c)



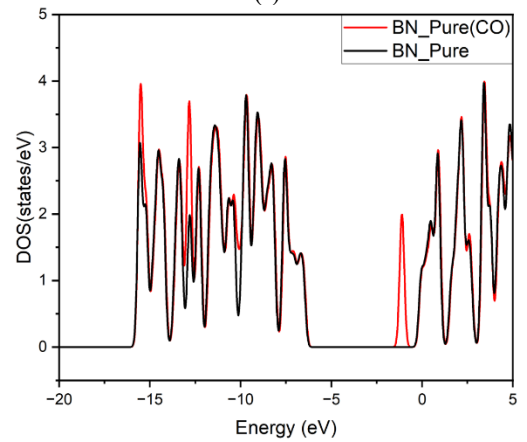
(d)



(e)



(f)



(g)

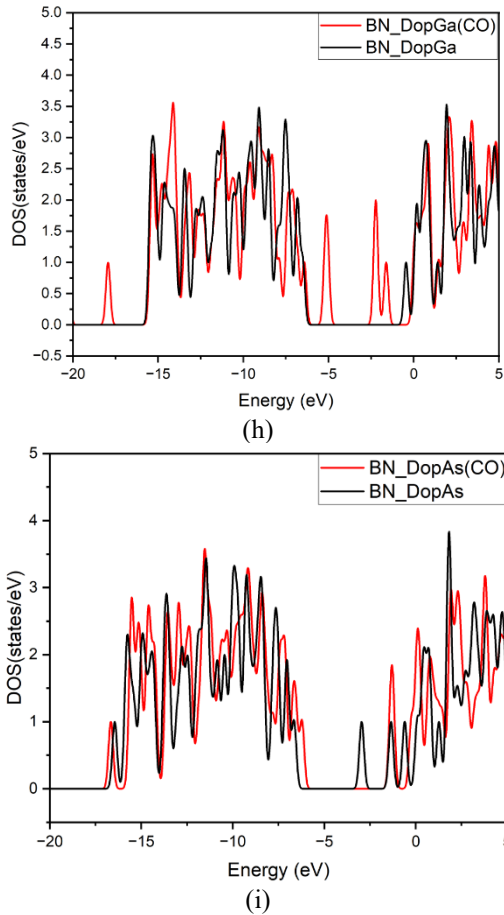


Figure 5. Density of states (DOS) for studied structures with and without CO

Molecular orbitals and their importance in chemical bonding are illustrated using the DOS spectra [31]. Figure 5 shows the difference in electron properties between gas-adsorbed G/S/BN NR and G/S/BN NR with gas absorption. It is not immediately obvious that the conductivity changes once CO adsorption occurs because, as it has been shown in Figure 5, the curves for G and BN Pure overlap near the Fermi level. When compared to G/BN_{pure}, S_{pure} characteristics for detecting CO gas are superior. A significant change in conductivity after absorbing CO gas is indicated by the huge change near the Fermi level, and the DOS change arises around (-5 to 0 eV) for G_{Doped} with (Ga, As) atoms. After CO gas adsorption, there is no discernible change in DOS with respect to the fraction of silicene doped with (Ga/As) atoms, while there is a small change when compared to pure S. Concerning BN Pure, a noticeable shift in DOS at (-1.1) suggests the existence of a minor degree of orbital hybridization. Following CO gas absorption, there is a little shift in DOS that manifests as (-6-0) for BN_{DopGa}, but no discernible shift in conductivity; in contrast, BN_{DopAs} shows a dramatic rise in conductivity following CO gas absorption.

3.5 UV-visible (Vis)

This section of the work investigates the kind of shifting blue or red by means of the influence of gas molecule on the optical characteristics of G-NR, S-NR, and BN-NR nano-ribbons. Determining the kind of shifting for adsorption gases on the surface of G-NR, S-NR, and BN-NR nano ribbons depends in great part on the optical computation. UV-Visible

Properties computed at basis set 6-31G using hybrid function B3LYP using TD-DFT approach. Figure 6 shows UV-visible spectra for adsorbed gas molecules respectively on the surface of pure, doped G-NR, S-NR, and BN-NR nano ribbons. Results show that blue shift exists in all BN-NR nano ribbons as well as pure G-NR. In the electromagnetic radiation, pure and doped S-NR shows red shifting. Strong interaction types $\pi \rightarrow \pi^*$. The highest wavelength in the interaction between the gas molecule and G-pure nano ribbon was (447.657) nm. Whereas pure and doped BN-NR is absorbed in the UV spectrum, S-NR pure and doped nano ribbons are all absorbed in the infrared area. It is obvious that strong chemical adsorption in CO causes a somewhat large change in UV-Visible spectrum.

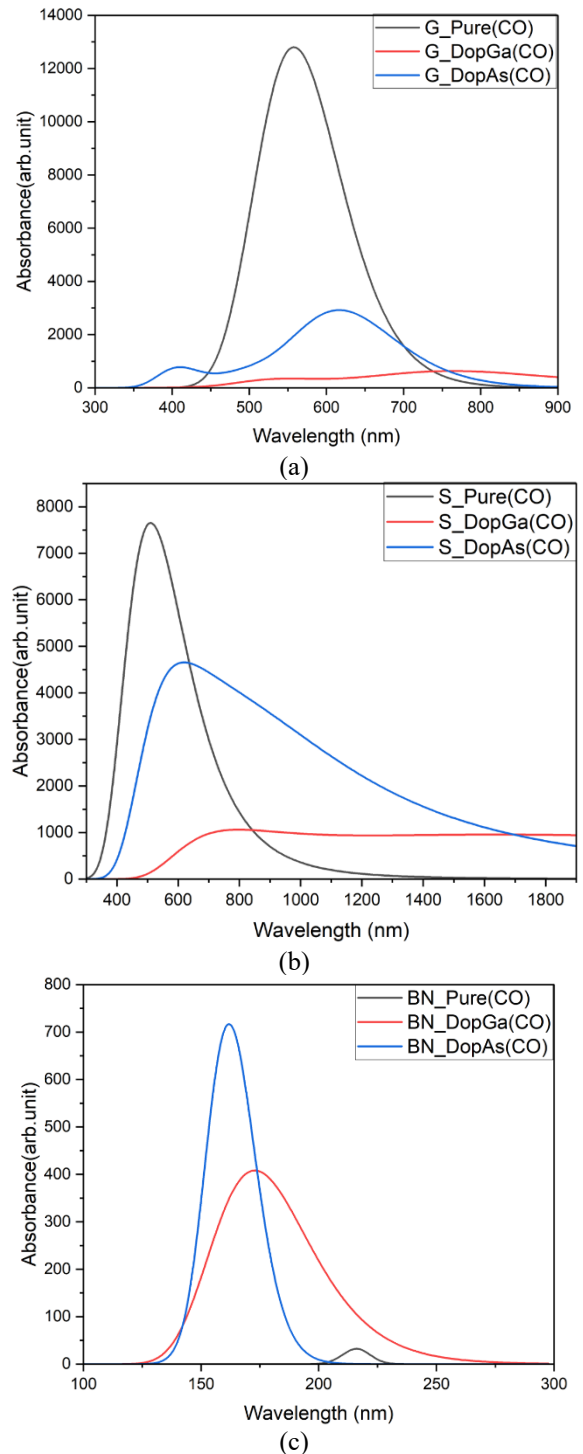
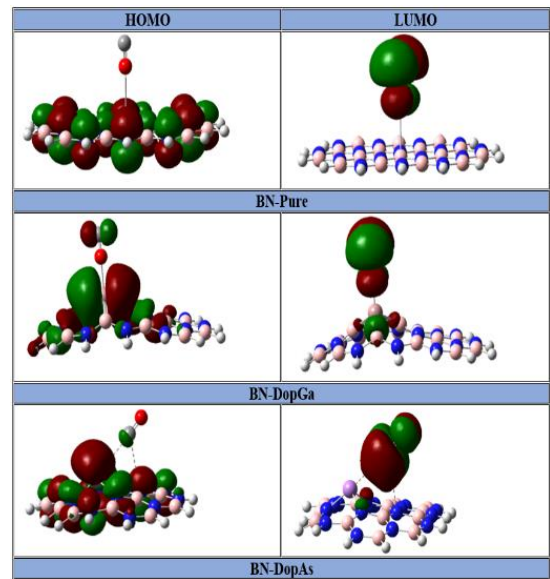


Figure 6. UV-Vis for studied structures with CO gas

3.6 Molecular Orbitals: HOMO and LUMO analysis

Figure 7 illustrates the distribution of the Highest Occupied Molecular Orbitals (HOMO) and the Lowest Unoccupied Molecular Orbitals (LUMO) for nanomaterials such as graphene, silicene, and boron nitride when doped with gallium (Ga) or arsenic (As), and their effect on CO gas adsorption. In the pure materials (G-Pure, S-Pure, BN-Pure), the electron density distribution is relatively balanced, whereas this distribution changes significantly upon doping with gallium or arsenic, enhancing interaction with CO gas. In the case of doped graphene (G-DopGa, G-DopAs) and doped silicene (S-DopGa, S-DopAs), a noticeable change in electron density distribution occurs around active sites, leading to increased reactivity and gas adsorption. Similarly, doped boron nitride (BN-DopGa, BN-DopAs) shows a significant enhancement in chemical adsorption due to changes in electron distribution. Overall, this indicates that doping these nanomaterials with Ga or As increases their sensitivity to CO gas detection by improving electronic and surface interactions.

Since the HOMO is a more fundamental orbital on charge transfer, invariably nano-ribbons follow from Since mostly it is found on the atom of a gas molecule, the charge transfer is maximum when atoms of gases are closer to the surface [32].



(c) BN-NR

Figure 7. Represents molecular orbital energy for CO gas adsorption

4. CONCLUSION

In this work, the adsorption mechanism for both pure and doped G/S/BN nano-ribbons onto the hazardous gas CO was investigated, along with the change in the electronic characteristics of G/S/BN-nano ribbons following doping with (Ga, As) atoms, using DFT.

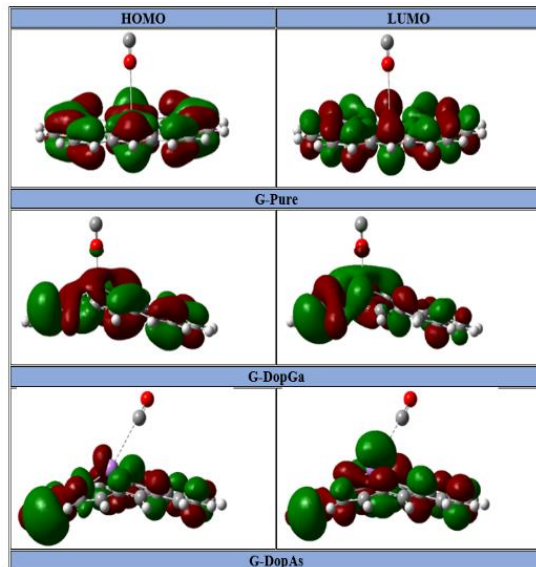
Based on DFT calculations, doping with Ga and As atoms enhances the electronic properties of G/S/BN, which affects the adsorption properties of CO gas, as the adsorption energy increases after doping while the adsorption energy of pure nano-ribbons on CO gas is low. This is consistent with the results of sensing, charge transfer, and molecular orbital distribution.

The best sensitivity, BN-DopeAs, reaches (202.941%), while GNR-DopGa has the heist adsorption energy (817.941). This indicates that BN doped with (Ga, As) atoms is the most appropriate for CO gas sensing applications form the studied models.

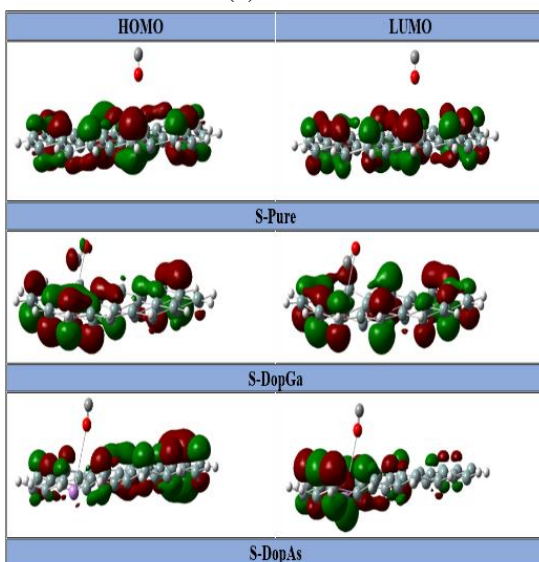
However, there are some limitations to consider, such as the simplification of the models used, which may not account for real-world defects, focusing on only one gas, and not considering the effects of temperature and pressure. To expand the study and improve practical outcomes, experimental studies should validate the theoretical predictions, explore the materials' sensitivity to a broader range of gases, examine the impact of environmental factors such as temperature and pressure, and investigate the effects of structural defects and edge configurations.

REFERENCES

- [1] Hjiri, M., El Mir, L., Leonardi, S.G., Pistone, A., Mavilia, L., Neri, G. (2014). Al-doped ZnO for highly sensitive CO gas sensors. *Sensors and Actuators B: Chemical*, 196: 413-420. <https://www.sciencedirect.com/science/article/abs/pii/S0925400514000859>.
- [2] Neri, G., Bonavita, A., Micali, G., Rizzo, G., Callone, E., Carturan, G. (2008). Resistive CO gas sensors based on



(a) G-NR



(b) S-NR

- In₂O₃ and InSnOx nanopowders synthesized via starch-aided sol-gel process for automotive applications. *Sensors and Actuators B: Chemical*, 132(1): 224-233. <https://doi.org/10.1016/j.snb.2008.01.030>
- [3] Xu, Y., Jiang, S.-X., Yin, W.-J., Sheng, W., Wu, L.-X., Nie, G.-Z., Ao, Z. (2020). Adsorption behaviors of HCN, SO₂, H₂S and NO molecules on graphitic carbon nitride with Mo atom decoration. *Applied Surface Science*, 501: 144199. <https://doi.org/10.1016/j.apsusc.2019.144199>
- [4] Lv, D., Shen, W., Chen, W., Wang, Y., Tan, R., Zhao, M., Song, W. (2023). Emerging poly (aniline co-pyrrole) nanocomposites by in-situ polymerized for high-performance flexible ammonia sensor. *Sensors and Actuators A: Physical*, 349: 114078. <https://doi.org/10.1016/j.sna.2022.114078>
- [5] Xu, Z., Cui, H., Zhang, G. (2023). Pd-Decorated WTe₂ Monolayer as a Favorable Sensing Material toward SF₆ Decomposed Species: A DFT Study. *ACS Omega*, 8(4): 4244-4250. <https://doi.org/10.1021/acsomega.2c07456>
- [6] Li, P., Zhang, Z. (2020). Self-Powered 2D Material-Based pH Sensor and Photodetector Driven by Monolayer MoSe₂ Piezoelectric Nanogenerator. *ACS Applied Materials & Interfaces*, 12(52): 58132-58139. <https://doi.org/10.1021/acsami.0c18028>
- [7] Neto, A.H.C., Guinea, F., Peres, N.M.R., Novoselov, K.S., Geim, A.K. (2009). The electronic properties of graphene. *Reviews of Modern Physics*, 81(1): 109. <https://journals.aps.org/rmp/abstract/10.1103/RevModPhys.81.109>
- [8] Tian, J., Li, G., He, W., Tan, K.B., Sun, D., Wei, J., Li, Q. (2023). Insight into the dynamic adsorption behavior of graphene oxide multichannel architecture toward contaminants. *Chinese Journal of Chemical Engineering*, 53: 124-132. <https://doi.org/10.1016/j.cjche.2021.12.029>
- [9] Zhao, J., Liu, H., Yu, Z., Quhe, R., Zhou, S., Wang, Y., Liu, C.C., Zhong, H., Han, N., Lu, J., Yao, Y., Wu, K. (2016). Rise of silicene: A competitive 2D material. *Progress in Materials Science*, 83: 24-151. <https://doi.org/10.1016/j.pmatsci.2016.04.001>
- [10] Zhu, H., Chen, X., Hong, Z., Huang, X., Meng, F.-B., Awais, M., Paramane, A. (2022). Ni-doped boron nitride nanotubes as promising gas sensing material for dissolved gases in transformer oil. *Materials Today Communications*, 33: 104845. <https://doi.org/10.1016/j.mtcomm.2022.104845>
- [11] Khudair, S., Jappor, H. (2020). Adsorption of gas molecules on graphene doped with mono and dual boron as highly sensitive sensors and catalysts. *Journal of Nanostructures*, 10(2): 217-229. https://jns.kashanu.ac.ir/article_106045.html
- [12] Liang, X., Ding, N., Ng, S.P., Wu, C.-M.L. (2017). Adsorption of gas molecules on Ga-doped graphene and effect of applied electric field: A DFT study. *Applied Surface Science*. <https://doi.org/10.1016/j.apsusc.2017.03.178>
- [13] Doust Mohammadi, M., Abdullah, H.Y., Biskos, G., Bhowmick, S. (2021). Effect of Al- and Ga-doping on the adsorption of H₂SiCl₂ onto the outer surface of boron nitride nanotube: A DFT study. *Comptes Rendus Chimie*. <https://doi.org/10.5802/crchim.87>
- [14] Bimukhanov, A.N., Aldongarov, A. (2023). A comparative study of DFT functionals and basis sets for describing the luminescent spectra of hexacoordinated silicon complexes. *Habarıřsý - Āl-Farabi atýndağý*. <https://doi.org/10.26577/rcph.2023.v84.i1.07>
- [15] Pitman, S.J., Ireland, R.T., Lempriere, F.A.R., McKemmish, L.K. (2023). Benchmarking basis sets for density functional theory thermochemistry calculations: Why unpolarized basis sets and the polarized 6-311G family should be avoided. *Journal of Physical Chemistry A*. <https://doi.org/10.1021/acs.jpca.3c05573>
- [16] Prasad, V.K., Otero-de-la-Roza, A., DiLabio, G.A. (2022). Small-basis set density-functional theory methods corrected with atom-centered potentials. *Journal of Chemical Theory and Computation*. <https://doi.org/10.1021/acs.jctc.2c00036>
- [17] Alsaati, S.A.A., Abdoon, R.S., Hussein, E.H., Abduljalil, H.M., Mohammad, R.K., Al-Seady, M.A., Jasim, A.N., Saleh, N.A.-H., Allan, L. (2024). Unveiling the potential of graphene and S-doped graphene nanostructures for toxic gas sensing and solar sensitizer cell devices: Insights from DFT calculations. *Journal of Molecular Modeling*, 30(6): 191. <https://doi.org/10.1007/s00894-024-05994-1>
- [18] Nguyen, D.K., Hoang, D.Q., Hoat, D.M. (2022). Exploring a silicene monolayer as a promising sensor platform to detect and capture NO and CO gas. *RSC Advances*, 12(16): 9828-9835. <https://doi.org/10.1039/d2ra00442a>
- [19] Kadhim, B.B., Muhsen, H.O. (2017). Infrared absorption and Raman spectra of BNNT-fluorouracil: A density functional theory study. *International Journal of Science and Research (IJSR)*, 6(8): 1690-1695. <https://doi.org/10.21275/ART20176361>
- [20] Peng, X., Liu, D., Zhao, F., Tang, C. (2022). Gas sensing properties of Mg-doped graphene for H₂S, SO₂, SOF₂, and SO₂F₂ based on DFT. *International Journal of Quantum Chemistry*, 122(22): e26989. <https://doi.org/10.1002/qua.26989>
- [21] Hu, W., Xia, N., Wu, X., Li, Z., Yang, J. (2014). Silicene as a highly sensitive molecule sensor for NH₃, NO, and NO₂. *Physical Chemistry Chemical Physics*, 16(15): 6957-6962. <https://doi.org/10.1039/c3cp55250k>
- [22] Tang, H., Xiang, Y., Zhan, H., Zhou, Y., Kang, J. (2023). DFT investigation of transition metal-doped graphene for the adsorption of HCl gas. *Diamond and Related Materials*, 136: 109995. <https://doi.org/10.1016/j.diamond.2023.109995>
- [23] Dovesi, R. (1996). Total energy and related properties. In *Quantum-Mechanical Ab-initio Calculation of the Properties of Crystalline Materials*, 67: 179-207. https://doi.org/10.1007/978-3-642-61478-1_11
- [24] Denis, P.A. (2014). Chemical reactivity and band-gap opening of graphene doped with gallium, germanium, arsenic, and selenium atoms. *ChemPhysChem*, 15(18): 3994-4000. <https://doi.org/10.1002/cphc.201402608>
- [25] Han, W.N., Yonezawa, K., Makino, R., Kato, K., Hinderhofer, A., Murdey, R., Shiraiishi, R., Yoshida, H., Sato, N., Ueno, N., Kera, S. (2013). Quantitatively identical orientation-dependent ionization energy and electron affinity of diindenoperylene. *Applied Physics Letters*, 103(25): 253301. <https://doi.org/10.1063/1.4850531>
- [26] Sabin, J.R., Trickey, S.B., Apell, S.P., Oddershede, J. (2000). Molecular shape, capacitance, and chemical hardness. *International Journal of Quantum Chemistry*,

- 77(1): 358-366. [https://doi.org/10.1002/\(SICI\)1097-461X\(2000\)77:1<358::AID-QUA35>3.0.CO;2-D](https://doi.org/10.1002/(SICI)1097-461X(2000)77:1<358::AID-QUA35>3.0.CO;2-D)
- [27] Milon, Roy, D., Ahmed, F. (2024). A first principle investigation of the CO gas adsorption property of pristine, cobalt (Co), and phosphorus (P) doped BN nanosheets. *Physica B: Condensed Matter*, 680: 415839. <https://doi.org/10.1016/j.physb.2024.415839>
- [28] Peyghan, A.A., Soltani, A., Pahlevani, A.A., Kanani, Y., Khajeh, S. (2013). A first-principles study of the adsorption behavior of CO on Al- and Ga-doped single-walled BN nanotubes. *Applied Surface Science*, 270: 25-32. <https://doi.org/10.1016/j.apsusc.2012.12.008>
- [29] Remsing, R.C., Sun, J., Waghmare, U.V., Klein, M.L. (2018). Bonding in the metallic molecular solid α -Gallium. *Figshare*. <https://doi.org/10.6084/m9.figshare.6662159>
- [30] Saleh, N.A.-H., Abduljalil, H.M., Abdoon, R.S. (2023). Study of adsorption energy for toxic gases (NH₃, Br₂) in pure and sulfur-doped graphene nano-ribbon. *Nucleation and Atmospheric Aerosols*. <https://doi.org/10.1063/5.0116788>
- [31] Babu, N.S. (2021). Donor–acceptor–donor (DAD) structural monomers as donor materials in polymer solar cells: A DFT/TDDFT approach. *Designed Monomers and Polymers*, 24(1): 330-342. <https://doi.org/10.1080/15685551.2021.1997178>
- [32] Beheshtian, J., Bagheri, Z., Kamfiroozi, M., Ahmadi, A. (2012). A theoretical study of CO adsorption on aluminum nitride nanotubes. *Structural Chemistry*, 23: 653-657. <https://doi.org/10.1007/s11224-011-9911-z>